ISSN impresa 0717-3644
ISSN online 0718-221X

Maderas. Ciencia y tecnología 2021 (23): 62, 1-14

DOI: 10.4067/s0718-221x2021000100462

EXPERIMENTAL AND NUMERICAL STUDY ON A NOVEL BAMBOO JOINT FOR FURNITURE CONSIDERING EFFECT OF LOADING TYPE ON MECHANICAL PARAMETERS USED IN FINITE ELEMENT METHOD

***Wengang Hu*[1,2,♠]**

https://orcid.org/0000-0001-8077-6324

***Binrui Chen*[2]**

https://orcid.org/0000-0002-1086-9864

***Xiaowen Lin*[2]**

https://orcid.org/0000-0002-2413-1369

***Huiyuan Guan*[2]**

https://orcid.org/0000-0002-8777-1689

ABSTRACT

The effect of loading type (tension, compression and bolt-bearing) on mechanical properties (elastic modulus, Poisson's ratio and ultimate strength) of Moso bamboo (*Phyllostachys heterocycla* var. *pubescens*) in longitudinal direction was evaluated in this study. In addition, experimental and numerical tests were conducted to evaluate withdrawal force capacity and bending moment resistances of a novel demountable bamboo-bolt joint considering effect of loading type on mechanical parameters used in finite element method. The results showed that loading type had significant effect on mechanical properties of Moso bamboo, especially, for ultimate strength; the values of mechanical properties evaluated in this study measured in tension were all much higher than those measured in bolt-bearing state and followed by compression accordingly; in tension, the tensile elastic modulus and Poisson's ratio measured at outer surface were bigger than those at inner surface, respectively; finite element method got more accurate results using the mechanical parameters measured in compression than those in tension and bolt-bearing states; the bamboo-bolt joint proposed in this study can be used in lightweight bamboo structures through improving the embedding strength of beech wood in bamboo culm. In conclusion, one should consider the loading type used to obtain the mechanical para meters inputted in finite element method. In addition, further studies will focus on effect of size and geometry of samples used to determine mechanical properties used in finite element method, and the method of improving embedding strength of beech wood in bamboo culm to increase withdrawal force capacity and bending moment resistances of the demountable bamboo-bolt joint proposed in this study.

Keywords: Bamboo-bolt joint, elastic modulus, finite element method, furniture, loading types, *Phyllostachys heterocycla*.

[1]Nanjing Forestry University, Co-Innovation Center of Efficient Processing and Utilization of Forest Resources, Nanjing, P.R. China.
[2]Nanjing Forestry University, College of Furnishings and Industrial Design, Department of furniture design, Nanjing, P.R. China.
[♠]Corresponding author: hwg@njfu.edu.cn
Received: 27.09.2020 Accepted: 17.06.2021

INTRODUCTION

Bamboo is a kind of natural biomass resource that can be used sustainably for its short harvest cycle, which has formed a unique cavity structure with high ratio of strength to weight. Bamboo is available in many tropical and subtropical areas which confer it attributes to become a renewable material as substitute of wood (Boran *et al*. 2016, Li *et al*. 2020). Nowadays, bamboo has been used in wide range of constructions and furniture. Generally, there are two approaches to applying bamboo into constructions and furniture, round bamboo and engineered bamboo (Razal *et al*. 2012, Sun *et al*. 2020).

In this work, we focused on mechanical properties of natural round bamboo used in lightweight bamboo structures and furniture based on finite element method (FEM). Hu *et al*. (2018) reported the mechanical properties of bolted joints in modern prefabricated round bamboo structures including single bolted joint, double bolted joint and strengthen joint with high-strength mortar. The results showed that the double bolted joint with the strengthen high-strength mortar could significantly improve the bearing capacity of the bolted joint. Pradhan *et al*. (2020) experimentally investigates the axial response of bamboo to steel connections under quasi-static reversed cyclic loading with three types of joints including plain bolted (type A), transversely confined by hose-clamps (type B), and transversely confined by hose-clamps and infilled with cement mortar (type C). The results showed that type B and C connections were superior to type A. In addition, Wang and Yang (2020) studied on load-capacity of dowel-type bolted bamboo joints by experimental and numerical methods. The results showed that ductile failure mode of bamboo occurred when large end spacing was applied, and the infilling grout can significantly increase the load-capacity of the dowelled joint. Villegas *et al*. (2015) proposed a new joint to assemble light structures of bamboo slats by using two small curved steel plates, a bolt, and a nut, which are used to apply high compressive deformation in the radial direction. Lefevre *et al*. (2019) presented a new design for a culm-to-culm joint is presented, based on the use of a custom-machined wooden block and metal hose-clamps.

The mechanical properties of bamboo are basic parameters used to evaluate the strength and stiffness of bamboo constructions and furniture based on numerical and analytic method. On mechanical properties of bamboo, many studies have been reported.

In case of microstructures and mechanical properties of bamboo, Chen *et al*. (2019) and Fei *et al.* (2019) did some works on this topic, such as microstructure of round bamboo and flattened bamboo. Shao *et al*. (2010) have successfully used the rule of mixtures, a simple model to describe aligned continuous fiber composites, to characterize the bamboo structure. Huang *et al*. (2012) investigated mechanical properties of single fibers isolated from Moso bamboo samples taken from plants between 0,5- and 8,5-year-old. The results showed that the effect of bamboo age on the modulus of elasticity (MOE) and tensile strength were not statistically significant. In addition, Ren *et al*. (2014) reported that the age did not have effect on these mechanical properties at 5 % significance level. Yu *et al*. (2014) tested elementary fibers from 11 bamboo species from China finding that bamboo fiber was much stronger and stiffer than wood fiber and comparable in extensibility due to its unique cell wall structure.

In case of mechanical properties of bamboo in macro scale, many researchers did abundant works. Table 1 summarizes some literatures studying on mechanical properties of bamboo in multi-scales, which indicated that MOE and tensile strength of bamboo fibers were obviously higher than those of fiber bundles and bamboo strips.

Table 1: Summary of tensile modulus of elasticity and strength of bamboo species reported in literatures.

Literatures	Tensile elastic modulus (GPa)			Tensile strength (GPa)		
	Strip	Fiber bundles	Fiber	Strip	Fiber bundles	Fiber
[1]		33,9	40		0,482	0,5817
[2]	19,85	16,5	34,62	0,30	0,29	0,93
[3]			43,67			1,61
[3]			35,98			1,40
[4]			32 - 36			1,2 - 1,7
[5]			36,7			1,55
[6]	9 - 27,4			0,115 - 0,309		
[7]				0,196		

[1]Shao *et al*. (2010), [2]Chen *et al*. (2015), [3]Ren *et al*. (2014), [4]Huang *et al*. (2012),[5]Yu *et al*. (2014), [6]Yu *et al*. (2008), [7]Handana *et al*. (2020).

Although mechanical properties of bamboo have been studied in multi-scales, some fundamental mechanical properties for engineering design of bamboo constructions and furniture based on FEM are still unclear. In this study, the main objective was to evaluate the effect of loading types on mechanical properties of Moso bamboo in macro scale for engineering usage. Specific works were conducted to 1) evaluate the ultimate strength of Moso bamboo in three loading types (tension, compression and bolt-bearing); 2) evaluate elastic moduli and Poisson's ratios of Moso bamboo in longitudinal direction under three loading types; 3) predict the withdrawal force capacity and bending moment resistances of a new bolt-bamboo joint based on finite element method (FEM) using mechanical parameters measured by three loading types; 4) validate the FEM experimentally through testing the withdrawal force capacity and bending moment resistances of the T-shaped bamboo-bolt joint samples.

MATERIALS AND METHODS

Materials

The main material used in this study was 3-years Moso bamboo (*Phyllostachys heterocycla* var. *pubescens*) cut at the middle of culm with outer diameter of 40 mm ± 2 mm and the thickness of wall 4 mm ± 0,5 mm. Figure 1 shows Moso bamboo material evaluated in this study and its corresponding microstructure photo. The density and moisture content (MC) of bamboo averaged 0,7 g/cm^3 and 9 %, respectively.

For the demountable bamboo-bolt joint proposed in this study, beech wood (*Fagus orientalis.* Lipsky) was used as an embedded material to connect bamboo and fastener. The density and MC of beech were 0,7 g/cm^3 and 12 %, respectively. In addition, mixture of 95 % urea formaldehyde (UF) resin powder and 5 % beech wood powder were used as bonding material to connect beech wood and bamboo. The ratio of mixture powder to water is 5:3. Figure 2 shows a fastener used to connect the T-shaped bamboo joint. The dimensions of the bolt measured 8 mm × 80 mm (diameter × length).

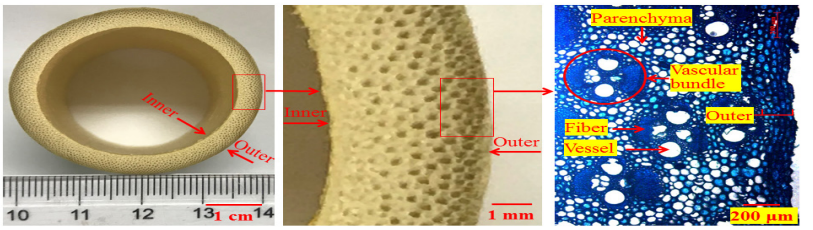

Figure 1: Moso bamboo evaluated in this study.

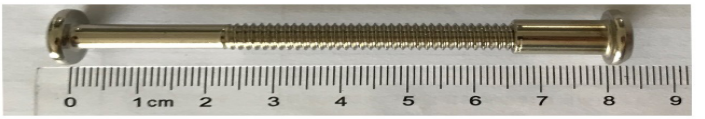

Figure 2: Fastener used to connect T-shaped bamboo joints.

Configurations of samples

Figure 3 shows the dimensions of samples used to determine mechanical properties of Moso bamboo evaluated in this study. The half-hole bolt-bearing sample (Figure 3a) was machined through drilling a hole with diameter of 8 mm on center of round bamboo and then cutting out half hole left a 80 mm round bamboo culm. The compressive sample (Figure 3b) was made up with a piece of 50 mm round bamboo culm with diameter of 40 mm. Figure 3c shows the tension sample machined by a CNC machine tool. In addition, the sample used to get the elastic modulus and Poisson's ratios were bamboo strip measured 180 mm long × 7 mm wide × 4 mm thick, half-hole bolt-bearing sample (Figure 3a) and compressive sample (Figure 3b).

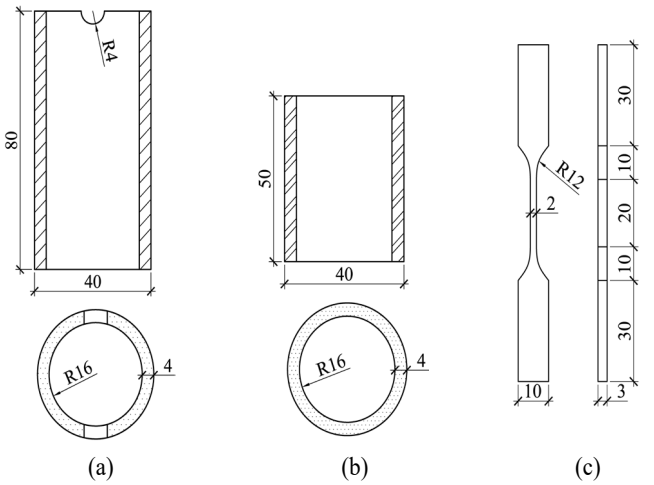

Figure 3: Configurations of samples used in this study (a) half-hole bolt-bearing sample, (b) compression sample, and (c) tension sample.

A novel demountable bamboo-bolt joint

Figure 4 shows the main procedure of assembling the novel demountable round bamboo T-shaped joint: a) prepare bamboo culm and beech wood tenon; b) connect the beech wood tenon and bamboo with bonding materials; c) insert the nut into beech wood tenon and assemble the bamboo culms with fastener; and d) finally get the demountable bamboo joint.

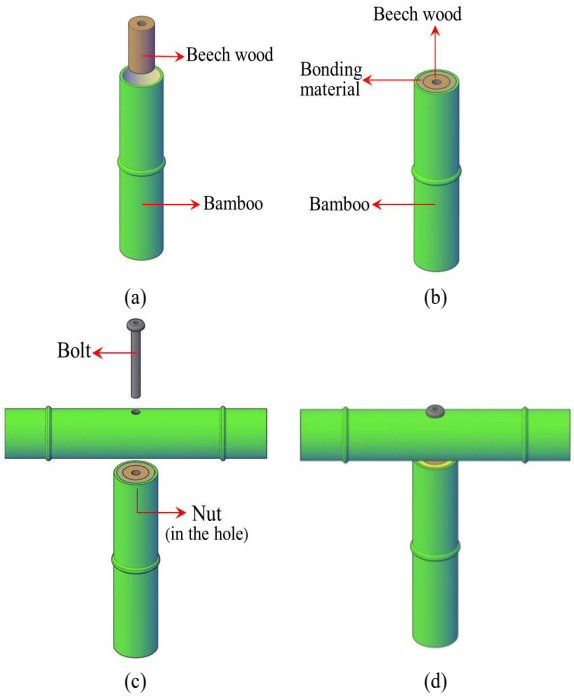

Figure 4: Assemble procedure of a new demountable bamboo T-shaped joint (a) prepare members to adhesive, (b) embed beech wood tenon into bamboo using bonding material, (c) connect the bamboo members with fastener, (d) a demountable bamboo-bolt joint.

Figure 5 shows the configurations of the demountable T-shaped bamboo-bolt joint proposed in this study. The dimensions of T-shaped bamboo joints were 200 mm long horizontal member and 200 mm long vertical member with 40 mm-diameter round bamboo internode culms. All samples were stored in the lab containing temperature of 23 ℃ ± 2 ℃ and relative humidity of 50 % ± 5 % before and during the tests.

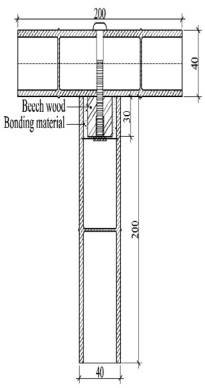

Figure 5: Dimensions of T-shaped demountable bamboo-bolt joint sample (unit: mm).

Testing methods

Figure 6 shows the setups of measuring compression strength of bamboo culm, tension strength of bamboo strip, and bolt-bearing strength (Eshaghi *et al*. 2013) of half-hole bamboo culm using a 20 kN universal test machine (SHIMDAZU, AGS-X, Japan). The loading rate was set at 1 mm/min until the failure of samples. Ten replications were repeated for each loading type. Equations used to calculate compression strength, tension strength and bolt-bearing strength were Equation 1, Equation 2 and Equation 3, respectively.

$$P_B = F / (2dt) \quad (1)$$

$$P_C = F / \left[\pi \left(D_1^2 - D_2^2 \right) \right] \quad (2)$$

$$P_T = F / (WT) \quad (3)$$

Where P_B is bolt-bearing strength of bamboo (MPa), F is maximum load (N), d is diameter of half-hole bolt-bearing sample (mm), t is thickness of bamboo wall (mm), Pc is compression strength of round bamboo (MPa), D_1 and D_2 are inner and outer diameters of round bamboo (mm), P_T is tension strength of bamboo (MPa), W and T are width and thickness of sample in tested part (mm).

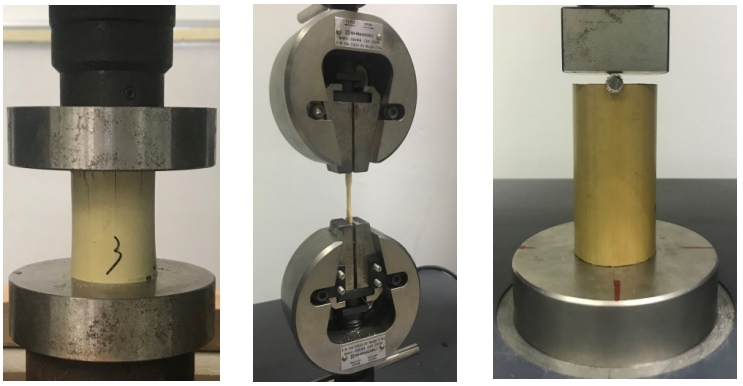

(a) (b) (c)

Figure 6: Setups of measuring ultimate strengths of bamboo (a) bolt-bearing strength, (b) compression strength, and (c) tension strength.

Elastic modulus and Poisson's ratio of Moso bamboo were also evaluated in this study. Figure 7 shows setups of measuring elastic modulus and Poisson's ratio of Moso bamboo in three loading types. They are tension method with bamboo strip, compression method with bamboo culm and bolt-bearing method with half-hole sample. In case of tension samples, the resistance strain gauges were attached at the center of samples both inner and outer surfaces. For compression samples, the strain gauges glued at the middle of outer surface of Moso bamboo. While for bolt-bearing samples, strain gauges were pasted 3 mm beneath the hole. A 20 kN universal test machine (SHIMDAZU, AGS-X, Japan) was used to conduct these tests. The loading speed was 1 mm/min, and the load was controlled within elastic stage referencing to the results of ultimate strength tests. Seven measurements were repeated for each loading type. Equation 4 and Equation 5 were used to calculate elastic moduli and Poisson's ratios, respectively.

$$E = \left(F_2 - F_1\right) / \left[S\left(\varepsilon_{y2} - \varepsilon_{y1}\right)\right] \quad (4)$$

$$\mu = \left(\varepsilon_{x2} - \varepsilon_{x1}\right) / \left(\varepsilon_{y2} - \varepsilon_{y1}\right) \quad (5)$$

Where F_1 and F_2 are initial load and final load (N), in this study, they are 500 N and 800 N for tension samples, 10000 N and 13000 N for compression samples, and 800 N and 1200 N for bolt-bearing samples. *S* is area of cross section of sample (mm^2). ε_{y1} and ε_{y2} are strains corresponding to F_1 and F_2 in longitudinal grain orientation of bamboo. ε_{x1} and ε_{x2} are strains corresponding to F_1 and F_2 perpendicular to longitudinal grain orientation of Moso bamboo.

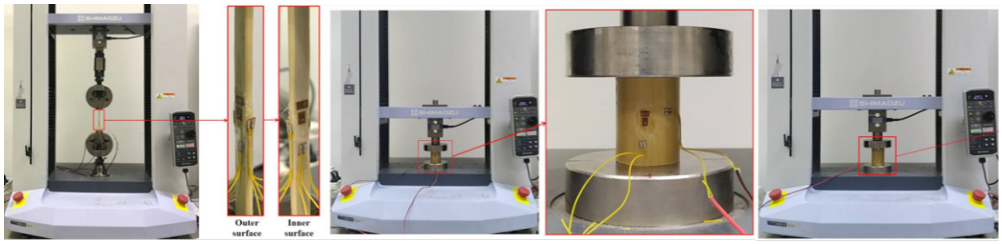

Figure 7: Setups for measuring elastic modulus and Poisson's ratio of Moso bamboo (a) tension method, (b) compression method, and (c) bolt-bearing method.

Figure 8 shows the setups for measuring withdrawal force capacity and bending moment resistance of T-shaped bamboo-bolt joints. Withdrawal force capacity and bending moment resistances of the bamboo-bolt joint were experimentally determined to compare with those of finite element models inputted with mechanical parameters measured in three loading types. Finally, the most accurate finite element model can be obtained, which indicated the best method to measure mechanical properties of Moso bamboo when using in FEM.

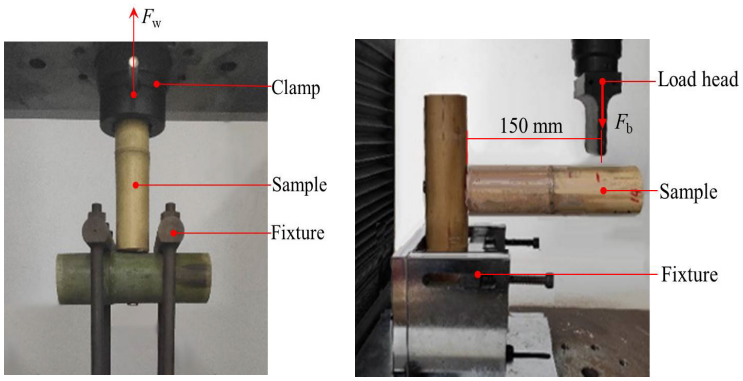

Figure 8: Setups for measuring (a) withdrawal force capacity and (b) bending moment resistance of bamboo joints.

Finite element models

As is known, mechanical properties are key parameters to numerically analyze the bamboo structures based on FEM. In this study, withdrawal force capacity and bending moment resistances of the T-shaped bamboo-bolt joint were analyzed to study effects of mechanical properties of Moso bamboo measured by three loading types on accuracy of FEM using nonlinear analysis method based on ABAQUS (ref). Figure 9 shows the finite element model of a T-shaped bamboo-bolt joint. Geometric dimensions of finite element model were as same as those shown in Figure 5. The elastoplastic strain-stress constitutive models of Moso bamboo measured through three loading types described above were used in the finite element model. The mechanical parameters of bolt were cited from Wang and Yang (2020), and the mechanical properties of beech wood obtained from Hu and Guan 2017a, Hu and Guan 2017b). The global size of element was approximately 5 mm, and C3D8 element type was specified to model. The embedding strength of beech wood in bamboo measured was 1,7 MPa which was specified to model through tangential contact behavior. The boundary constraints were referred to setups of withdrawal and bending tests shown in Figure 8.

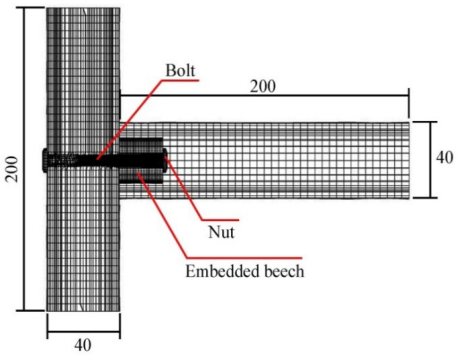

Figure 9: Finite element model of T-shaped bamboo-bolt joint.

Statistical analysis

The effects of bamboo layer (inner and outer surfaces) on elastic modulus and Poisson's ratio of Moso bamboo in tension state, and the effects of loading types on ultimate strength, elastic modulus and Poisson's ratios in three loading types were analyzed using the analysis of variance (ANOVA) with general linear model (GLM) procedure. Mean comparisons using the protected least significant difference (LSD) multiple comparison procedure was performed if any significant interaction was identified, otherwise, the main effects were concluded. All statistical analyses were performed at the 5 % significance level.

RESULTS AND DISCUSSION

Mechanical properties

Figure 10 and Figure 11 show the typical deformation and load curves and typical failure modes of three loading types, respectively. It can be found that the failure modes of bamboo samples tended to be brittle failure, especially for tension samples. In case of compression and bolt-bearing samples, the final failure was caused by the split of bamboo samples. For tension sample, the failure resulted from the damage of inner surface of bamboo since the strength of inner surface was smaller than outer surface. The outer part separated from the bamboo samples which had higher stiffness and strength than inner part of bamboo (Yu *et al*. 2008).

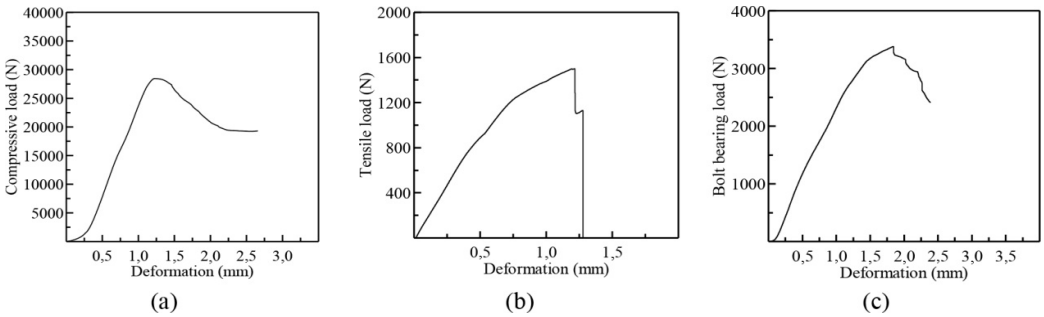

Figure 10: Deformation and load curves under states of (a) compression, (b) tension, and (c) bolt-bearing.

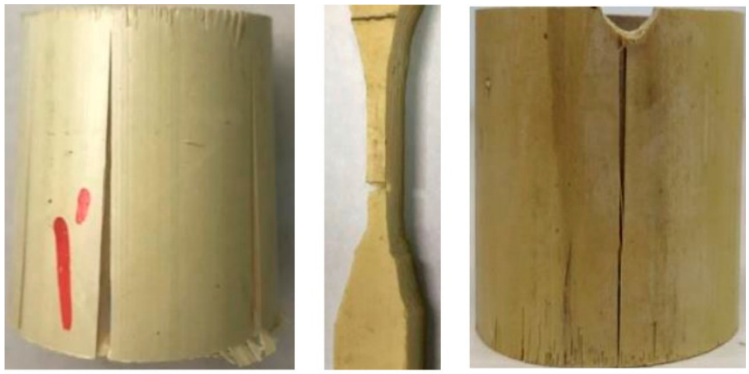

Figure 11: Failure modes of tested samples evaluated in this study (a) compression sample, (b) tension sample, and (c) half-hole bolt-bearing sample.

Table 2 shows the ANOVA results of elastic moduli and Poison's ratios of Moso bamboo measured in tension state, which indicated that bamboo layer (inner and outer) had a significant effect on Poisson's ratio and elastic modulus at 5 % significance level. Previous study (Yu *et al*. 2008) also reported that layer had significant effect on physical and mechanical properties of Moso bamboo.

Table 2: Summary of ANOVA results of elastic modulus and Poison's ratio of bamboo measured at inner and outer surface through general linear model procedure performed on one factor, bamboo surface.

Sources	Elastic modulus		Poisson's ratio	
Bamboo layers	*F*-value	*p*-value	*F*-value	*p*-value
	1,911	0,023	9,798	0,009

Table 3 shows ANOVA results of effect of loading type on mechanical properties of Moso bamboo suggesting that the effect of loading type on elastic modulus, strength and Poisson's ratio are all significant at 5 % significance level based on the *p*-values, especially for strength of bamboo, since the *F*-values of strength is much bigger than those of elastic modulus and Poisson's ratio.

Table 3: Summary of ANOVA results of the effect of loading type on mechanical properties of Moso bamboo.

Source	Mechanical property	*F*-value	*p*-value
Loading type	Strength	1026,94	<0,05
	Elastic modulus	47,16	<0,05
	Poisson's ratio	6,622	<0,05

To further study these significant differences, mean comparisons were conducted using LSD method, and the results were shown in Table 4. In case of elastic modulus, the value measured in tension state was much higher than those measured in compression and bolt-bearing states, and the elastic modulus measured in compression state was very close to the one measured in bolt-bearing state. For Poisson's ratio, the value measured through tension method at outer surface of Moso bamboo was significantly higher than those measured at inner surface and measured by compression method, and the post two values were in a good agreement. Comparing strengths of Moso bamboo measured through three loading types, it can be found that the tensile strength was much higher than those of bolt-bearing strength and followed by compressive strength. The reasons were that strengths of bamboo dependent on cell walls, especially on secondary wall (S2). According to the studies (Osorio *et al*. 2018), micro fibrils of S2 oriented at an angle of ± 30° compared with longitudinal direction of bamboo, which makes the cell wall easily be compressed rather than tension. Therefore, the tensile elastic modulus and tensile strength of bamboo in longitudinal were all much higher than those measured in compression loading state. In addition, the tensile failure was mainly caused by fracture of fiber, while the compressive failure resulted from the fibers crash and separations (Figure 11) caused by fracture of Parenchyma tissue. According to previous studies (Shao *et al*. 2010, Ren *et al*. 2014), the strength of Parenchyma tissue was much lower than elementary fiber and fiber bundles, which caused the fibers separated easily when subjected to compressive load in axial direction.

Table 4: Mean comparison of elastic moduli and strength of bamboo for different loading types.

Loading type	Elastic modulus (MPa)		Poisson's ratio	Strength (MPa)
Tension	outer	8700 (8,89) A	0,3837 (23,95) A	210 (6,04) A
	inner	8178 (7,74) A	0,2530 (24,20) B	
Compression	4734(20,18) B		0,2447 (18,63) B	37 (3,83) C
Bolt-bearing	4981(16,61) B		---	55 (13,21) B

Note: "---" means that the value is not available; the values in parenthesis are coefficient of variance (COV). The values in each column not followed by a common letter are significantly different one from the others at 5 % significance level.

Withdrawal force capacity and bending moment resistances of bamboo-bolt joint

Figure 12 shows the failure modes of T-shaped bamboo-bolt joint when subjected to withdrawal and bending loads. It can be found that the failure modes of samples subjected withdrawal and bending loads mainly resulted from the loose of embedded beech, which indicated that embedding strength of beech wood in Moso bamboo dominated the withdrawal force capacity and bending moment resistance of bamboo-bolt joint proposed in this study.

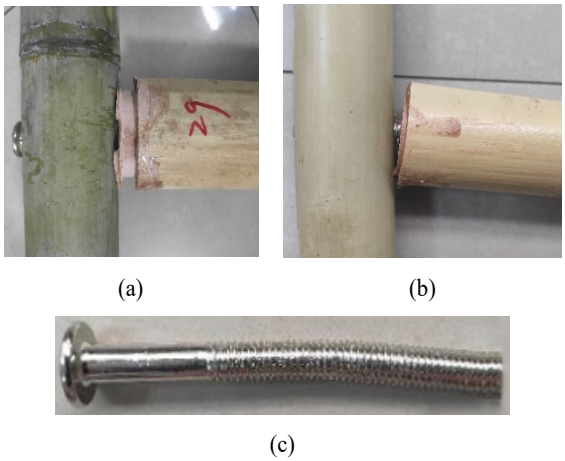

Figure 12: Failure modes of T-shaped bamboo joint (a) withdrawal force capacity, (b) bending moment resistance and (c) bent bolt.

Figure 13 shows stress distributions of the bamboo-bolt joint and bolt subjected to withdrawal load. The failure of finite element model was because of the embedded beech wood pulled out from bamboo, which was consistent with failure modes of experiment shown in Figure 12. In addition, the stress mainly concentrated on the holes of bamboo and bolt based on the stress distributions of bolt.

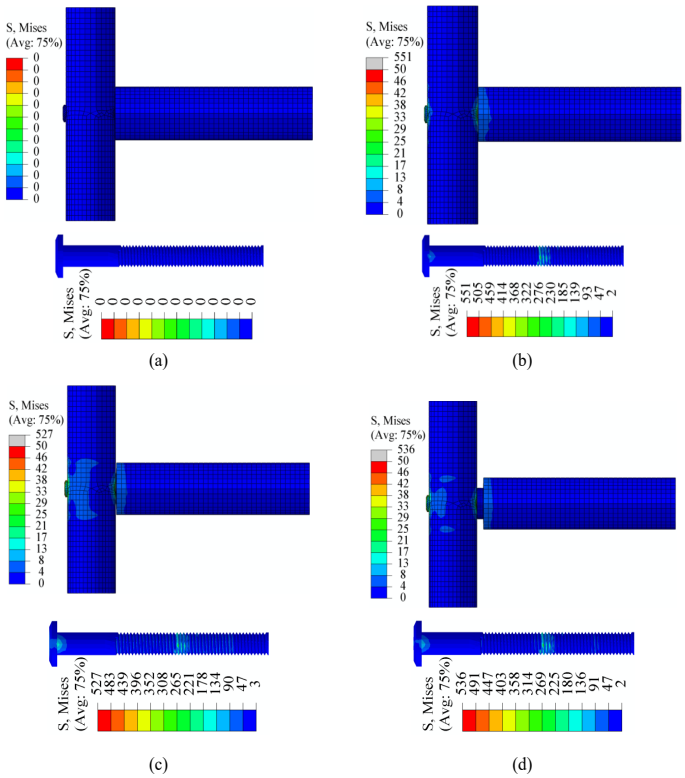

Figure 13: Stress distributions of bolted bamboo joint during withdrawal load processes a) initial state, b) preliminary load state, c) maximum load state and d) failure state.

Figure 14 presents the stress distributions of T-shaped bamboo-bolt joint and bolt when subjected to bending load. The failure of the sample mainly resulted from the loose of embedded beech wood and bent of bolt. The maximum stress was occurred at bent part of bolt.

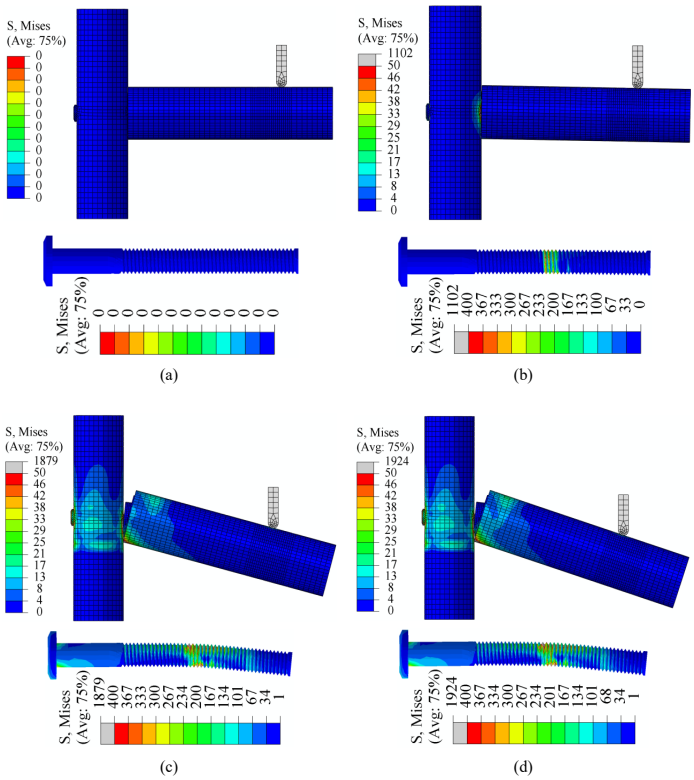

Figure 14: Stress distributions of bamboo-bolt joint during bending load processes a) initial state, b) preliminary load state, c) maximum load state and d) failure state.

Table 5 summarize the experimental results of withdrawal force capacity and bending moment resistances compared with FEM using mechanical parameters measured in three loading types. The results indicated that the both withdrawal force capacity and bending moment resistances of bamboo-bolt joint predicted using FEM were higher than observed ones. The reason why FEM overestimated the withdrawal force capacity and bending moment resistances of bamboo-bolt joint was that the assemblies of tested samples were not as tight as finite element mode. In addition, the accuracies of FEM inputted mechanical parameters measured in compression and bolt-bearing states were higher than those measured in tension state. Therefore, it is recommended that the mechanical properties measured in compression state are more suitable to be applied to FEM in this study. Furthermore, it can be concluded that in order to get more accurate simulation results based on FEM, the selection of mechanical properties should consider the real loading conditions, size and geometry effects on mechanical properties (Carpinteri and Pugno 2005, Hu *et al*. 2019).

Table 5: Comparisons of withdrawal force capacity and bending moment resistance of bamboo-bolt joint between experiment and FEM using mechanical parameters measured in three loading types.

Loading type	Withdrawal force capacity (N)			Bending moment resistance (N)		
	FEM	Observed	Ratio	FEM	Observed	Ratio
Tension	1558,27	1311 (33,3)	1,19	414,89	293,2 (32,4)	1,42
Compression	1487,22		1,13	383,72		1,31
Bolt-bearing	1494,40		1,14	384,47		1,31

CONCLUSIONS

In this study, the effect of loading type on mechanical properties (elastic modulus, Poisson's ratio and strength) of Moso bamboo (*Phyllostachys heterocycla* var. *pubescens*) in longitudinal direction was studied, and these mechanical parameters were used to predict withdrawal force capacity and bending moment resistances of a novel bamboo-bolt joint based on finite element method (FEM). Following conclusions were drawn:

Loading types had significant effect on mechanical properties of Moso bamboo, especially, for ultimate strength. The values of mechanical properties measured in tension state were all much higher than those measured in bolt-bearing state and followed by compression state accordingly.

FEM got more accurate results when using the mechanical properties measured in compression and bolt-bearing states compared with tension state, which indicated that one should consider the method of obtaining the mechanical parameters inputted into finite element model.

The bamboo-bolt joint proposed in this study can be used in lightweight bamboo structures and the strength of joint can be improved through increasing the embedding strength of beech wood in bamboo culm.

In future study, the effects of size and geometry of sample used to determine mechanical properties of bamboo will be evaluated to get more accurate finite element analysis. In addition, further studies will also focus on improving embedding strength of beech wood in bamboo culm to increase withdrawal force capacity and bending moment resistances of the bamboo-bolt joint proposed in this study.

ACKNOWLEDGEMENTS

This study was financed by Scientific Research Foundation of Metasequoia teacher (163104060), and a project funded by A Project Funded by the National First-class Disciplines (PNFD).

REFERENCES

Boran, S.; Donmez Çavdar**, A.; Barbu, M.C. 2016.** Evaluation of bamboo as furniture material and its furniture designs. *Pro Ligno* 9(4): 811-819. http://www.proligno.ro/ro/articles/2013/4/Boran_final.pdf

Carpinteri, A.; Pugno, N. 2005. Are scaling laws on strength of solids related to mechanics or to geometry. *Nat Mater* 4: 421-423. https://doi.org/10.1038/nmat1408

Chen, H.; Zhang, Y.; Han, J.; Zhong, T.; Wang, G. 2019. A comparative study of the microstructure and water permeability between flattened bamboo and bamboo culm. *J Wood Sci* 65: 44. https://doi.org/10.1186/s10086-019-1842-0

Chen, H.; Cheng, H.; Wang, G.; Yu, Z.X.; Shi, S.Q. 2015. Tensile properties of bamboo in different sizes. *J Wood Sci* 61: 552-561. https://doi.org/10.1007/s10086-015-1511-x

Eshaghi, S.; Faezipour, M.; Taghiyari, H.R. 2013. Investigation on lateral resistance of joint made with drywall and sheet metal screws in bagasse particleboard and comparison with that of commercial MDF. *Maderas-Cienc Tecnol* 15(2): 127-140. http://dx.doi.org/10.4067/S0718-221X2013005000011

Fei, B.; Liu, R.; Liu, X.; Chen, X.; Zhang, X. 2019. A review of structure and characterization methods of bamboo pits. *J Forest Eng* 4(2): 13-18. https://doi.org/10.13360/j.issn.2096-1359.2019.02.002

Handana, M.A.P.; Surbakti, B.; Harisdani, D.D.; Karolina, R.; Rizki, T.F. 2020. Compressive and tensile strengths of bamboo species. *IOP Conference Series: Earth and Environmental Science* 519: 012026. https://doi.org/10.1088/1755-1315/519/1/012026

Hu, W.; Guan, H. 2017a. Study on elastic constants of beech in different stress states. *J Forest Eng* 2(6): 31-36. https://doi.org/10.13360/j.issn.2096-1359.2017.06.006

Hu, W.; Guan, H. 2017b. Investigation on withdrawal capacity of mortise and tenon joint based on friction properties. *J Forest Eng* 2(4): 158-162. https://doi.org/10.13360/j.issn.2096-1359.2017.04.025

Hu, W.; Wan, H.; Guan, H. 2019. Size effect on the elastic mechanical properties of beech and its application in finite element analysis of wood structures. *Forests* 10(9): 783. https://doi.org/10.3390/f10090783

Hu, H.; Yang, J.; Wang, F.; Zhang, Y. 2018. Mechanical properties of bolted joints in prefabricated round bamboo structures. *J Forest Eng* 3(5): 128-135. http://doi.org/10.13360/j.issn.2096-1359.2018.05.020

Huang, Y.H.; Fei, B.H.; Yu, Y.; Zhao, R.J. 2012. Plant age effect on mechanical properties of Moso bamboo (Phyllostachys heterocycla var. pubescens) single fibers. *Wood Fiber Sci* 44(2): 196-201. https://wfs.swst.org/index.php/wfs/article/view/415

Lefevre, B.; West, R.; O'Reilly, P.; Taylor, D. 2019. A new method for joining bamboo culms. *Eng Struct* 190: 1-8. https://doi.org/10.1016/j.engstruct.2019.04.003

Li, H.; Xuan, Y.; Xu, B.; Li, S. 2020. Bamboo application in civil engineering field. *J Forest Eng* 5(6): 1-10. https://doi.org/10.13360/j.issn.2096-1359.202003001

Osorio, L.; Trujillo, E.; Lens, F.; Ivens, J.; Verpoest, I.; Van Vuure, A.W. 2018. In-depth study of the microstructure of bamboo fibres and theirrelation to the mechanical properties. *J Reinf Plast Comp* 37(17): 1099-1113. https://doi.org/10.1177/0731684418783055

Pradhan, N.P.N.; Paraskeva, T.S.; Dimitrakpoulos, E.G. 2020. Quasi-static reversed cyclic testing of multi-culm bamboo members with steel connectors. *J Build Eng* 27: 100983. https://doi.org/10.1016/j.jobe.2019.100983

Razal, R.A.; Dolom, P.C.; Palacpac, A.B.; Villanueva, M.M.B.; Camacho, S.C.; Alipon, M.B.; Bantayan, R.B.; Malab, S.C. 2012. *Mainsteaming engineered-bamboo products for construction and furniture*. Philippine Council for Agriculture, Aquatic, and Natural Resources Research and Development: Los Baños, Laguna, Philippines. ISBN: 978-971-579-061-1. http://doi.org/10.13140/RG.2.1.3490.9200

Ren, D.; Yu, Z.X.; Li, W.J.; Wang, H.K.; Yan, Y. 2014. The effect of ages on the tensile mechanical properties of elementary fibers extracted from two sympodial bamboo species. *Ind Crop Prod* 62: 94-99. https://doi.org/10.1016/j.indcrop.2014.08.014

Shao, Z.P.; Fang, C.H.; Huang, S.X.; Tian, G.L. 2010. Tensile properties of Moso bamboo (Phyllostachys pubescens) and its components with respect to its fiber-reinforced composite structure. *Wood Sci Technol* 44: 655-666. https://doi.org/10.1007/s00226-009-0290-1

Sun, L.; Bian, Y.; Zhou, A.; Zhu, Y. 2020. Study on short-term creep property of bamboo scrimber. *J Forest Eng* 5(2): 69-75. http://doi.org/10.13360/j.issn.2096-1359.201905021

Villegas, L.; Morán, R.; García, J.J. 2015. A new joint to assemble light structures of bamboo slats. *Constr Build Mater* 98: 61-68. http://dx.doi.org/10.1016/j.conbuildmat.2015.08.113

Wang, F.L.; Yang, J. 2020. Experimental and numerical investigations on load-carrying capacity of dowel-type bolted bamboo joints. *Eng Struct* 209: 109952. https://doi.org/10.1016/j.engstruct.2019.109952

Yu, Y.; Wang, H.; Lu, F.; Tian, G.L.; Lin, J.G. 2014. Bamboo fibers for composite applications: a mechanical and morphological investigation. *J Mater Sci* 49: 2559-2566. https://doi.org/10.1007/s10853-013-7951-z

Yu, H.; Jiang, Z.; Hse, C.Y.; Shupe, T.F. 2008. Selected physical and mechanical properties of moso bamboo (phyllostachys pubescens). *J Trop For Sci* 20(4): 258-263. https://www.jstor.org/stable/23616702?seq=1